BIOLOGY OF REPRODUCTION (2015) **93**(4):90, 1–11
Published online before print 2 September 2015.
DOI 10.1095/biolreprod.114.123638

Lgr4 Controls Specialization of Female Gonads in Mice[1]

Masae Koizumi,[3,5] Kazunori Oyama,[3] Yukiko Yamakami,[3] Tomoyo Kida,[3] Ryo Satoh,[4] Shigeki Kato,[3] Shizu Hidema,[3] Tomoyuki Oe,[4] Takaaki Goto,[4] Hans Clevers,[6] Akihiro Nawa,[5] and Katsuhiko Nishimori[2,3]

[3]*Laboratory of Molecular Biology, Graduate School of Agricultural Science, Tohoku University, Sendai, Japan*
[4]*Department of Bio-analytical Chemistry, Graduate School of Pharmaceutical Sciences, Tohoku University, Sendai, Japan*
[5]*Department of Obstetrics and Gynecology, Ehime University School of Medicine, Toon, Japan*
[6]*Hubrecht Institute, Royal Netherlands Academy of Arts and Sciences, University Medical Center Utrecht, Utrecht, The Netherlands*

ABSTRACT

Leucine-rich repeat-containing G protein-coupled receptor 4 (*Lgr4*) is a type of membrane receptor with a seven-transmembrane structure. LGR4 is homologous to gonadotropin receptors, such as follicle-stimulating hormone receptor (*Fshr*) and luteinizing hormone/choriogonadotropin receptor (*Lhcgr*). Recently, it has been reported that *Lgr4* is a membrane receptor for R-spondin ligands, which mediate Wnt/beta-catenin signaling. Defects of R-spondin homolog (*Rspo1*) and wingless-type MMTV integration site family, member 4 (*Wnt4*) cause masculinization of female gonads. We observed that *Lgr4*$^{-/-}$ female mice show abnormal development of the Wolffian ducts and somatic cells similar to that in the male gonads. *Lgr4*$^{-/-}$ female mice exhibited masculinization similar to that observed in *Rspo1*-deficient mice. In *Lgr4*$^{-/-}$ ovarian somatic cells, the expression levels of lymphoid enhancer-binding factor 1 (*Lefl*) and Axin2 (*Axin2*), which are target genes of Wnt/beta-catenin signaling, were lower than they were in wild-type mice. This study suggests that *Lgr4* is critical for ovarian somatic cell specialization via the cooperative signaling of *Rspo1* and Wnt/beta-catenin.

female reproductive tract, sex differentiation, steroid hormones/steroid hormone receptor, testosterone

INTRODUCTION

Leucine-rich repeat-containing G protein-coupled receptor (*Lgr*) 4 structurally belongs to the large G protein-coupled, seven-transmembrane protein family and has high homology with glycoprotein hormone receptors, including follicle-stimulating hormone receptor (*Fshr*), luteinizing hormone/choriogonadotropin receptor (*Lhcgr*), and thyroid-stimulating hormone receptor (*Tshr*) [1]. The gonadotropin receptors (FSHR and LHR) are type A LGRs and have indispensable roles in reproductive function [2–5]. LGR7 and LGR8 are type C LGRs and have important roles in reproduction-related functions [6–8]. LGR4, LGR5, and LGR6 are type B LGRs [1]. Type B LGRs are related to development and homeostasis in various organs [9–16]. Previously we generated *Lgr4* conditional knockout (KO) mice by using the *Keratin5-Cre* mouse model (*Lgr4*$^{tm1.1Knis}$/*Lgr4*$^{tm1.1Knis}$; Tg [KRT5-cre] 1Tak) [10]. These female mice exhibited subfertility with impaired embryonic development in the oviduct during early pregnancy [11]. We demonstrated that LGR4 is required for postnatal development of the uterine gland. *Lgr4*^{K5KO} mice lost the ability to undergo induced decidualization, which is characterized by proliferation and differentiation of uterine stromal cells to support embryo implantation [12]. LGR4 and its homolog, LGR5, are receptors of RSPO1–4, secreted Wnt pathway agonists, amplifying canonical Wnt signaling [13–15]. These studies suggest that the LGR4 family receptors are active components of RSPO-induced Wnt/β-catenin activation.

There are no apparent morphological differences between female and male mammalian genitalia during early fetal stages. The genitalia consist of undifferentiated germinal glands and two types of ducts (Wolffian ducts and Müllerian ducts). The Müllerian ducts are the anlagen of the oviducts, uterus, cervix, and upper portion of the vagina, whereas the Wolffian ducts are those of the epididymis, vas deferens, and seminal vesicles. Sexual differentiation of the duct in the fetal stage is dependent on the differentiation of gonadal somatic cells and subsequent synthesis of male hormones. In male mice, the sex-determining region of Chr Y (*Sry*) is expressed at Embryonic Day (E) 10.5 (10.5 days postcoitum) in the bipotential gonads. After the onset of *Sry* expression, SRY-box 9 (*Sox9*) is upregulated and Sertoli cells differentiate, which is followed by the differentiation of Leydig cells. Anti-Müllerian hormone (AMH) and male-specific steroid hormones (androgens) are produced by the male gonads. Müllerian ducts degenerate in response to AMH secretion, the Wolffian ducts mature, and the male glands differentiate into testes [17, 18]. In females, the Müllerian ducts develop in the absence of AMH and androgens. The Wolffian ducts degenerate, and the female gonads differentiate into ovaries [19]. The differentiation of ovarian somatic cells during the fetal stage is poorly understood. Previous studies have proposed that female sexual differentiation is determined by the absence of the expression of testis-determining genes, including SRY [20]. However, it was recently reported that mutations in some genes lead to masculinization of mammalian female gonads. Forkhead box L2 (*Foxl2*) is a forkhead transcription factor expressed in pregranulosa cells of early fetal gonads. Mutations in *Foxl2* in humans lead to blepharophimosis/ptosis/epicanthus inversus syndrome, an autosomal dominant genetic disorder characterized by drooping eyelids and/or premature ovarian failure in

[1]Supported by a Grant-in-Aid for Exploratory Research from the Japan Society for the Promotion of Science, Grants-in-Aid for Scientific Research on Innovative Areas, and research fellowships of the Japanese Society for the Promotion of Science for Young Scientists to K.O.
[2]Correspondence: Katsuhiko Nishimori, Laboratory of Molecular Biology, Tohoku University Graduate School of Agricultural Science, Tsutsumidori-Amamiyamachi 1-1, Aoba-ku, Sendai-city 981-8555, Miyagi-pref., Japan. E-mail address: knishimori@m.tohoku.ac.jp

Received: 27 July 2014.
First decision: 14 August 2014.
Accepted: 18 August 2015.

eISSN: 1529-7268 http://www.biolreprod.org
ISSN: 0006-3363

women [21]. Loss-of-function *Foxl2* in mice causes transdifferentiation of granulosa cells to Sertoli-like cells after birth [22, 23]. Furthermore, Wnt/beta-catenin signaling-associated genes, *Wnt4* and *Rspo1*, are known to be important for female sex determination [24]. Disruption of *RSPO1* in humans is responsible for XX sex reversal associated with palmoplantar hyperkeratosis and predisposition to skin squamous cell carcinoma [25]. Loss-of-function mutations in *Rspo1* and *Wnt4* in mice lead to a partial female-to-male sex reversal of gonads, characterized by the upregulation of steroidogenic enzymes, transdifferentiation of precursors of supporting somatic cells, and reduced germ cell viability [26–28]. Although LGR4 acts as a receptor of RSPO1 and promotes Wnt/beta-catenin signaling, its function in fetal female reproductive organs is unclear. Here, we show that *Lgr4* functions in controlling the development of fetal female gonads in relation to Wnt/beta-catenin signaling. We also present data on *Lgr4* in adult female gonads.

MATERIALS AND METHODS

Animals

The care and use of mice in this study were approved by the Institutional Animal Care and Use Committee of Tohoku University (Sendai, Japan). Two mouse strains were used, with an EGFP knockin reporter allele ($Lgr4^{tm1[cre/ERT2]Cle}$) [14] and an *Lgr4 Ex18* KO allele via loxP sites ($Lgr4^{tm1.2Knis}$) [16]. To identify cells with LGR4 expression in gonads, $Lgr4^{tm1(cre/ERT2)Cle}/Lgr4^{+}$ (referred to as $Lgr4^{EGFP\text{-}IRES\text{-}CreERT2/+}$) mice were used [14]. To harvest $Lgr4^{EGFP\text{-}IRES\text{-}CreERT2/+}$ embryos, $Lgr4^{EGFP\text{-}IRES\text{-}CreERT2/+}$ male and $Lgr4^{+/+}$ female mice were housed together overnight. The morning of the day that the female was plugged was considered E0.5. Embryos were harvested at E14.5 following timed mating. For functional analysis, the effect of *Lgr4* loss of function was assessed using $Lgr4^{tm1.2Knis}/Lgr4^{tm1.2Knis}$ mice [16]. We defined the $Lgr4^{Floxed}$ allele ($Lgr4^{tm1.1Knis}$) as that with the intact targeting vector. To obtain the *Lgr4* KO or null allele, $Lgr4^{tm1.1Knis}/Lgr4^{tm1.1Knis}$ ($Lgr4^{fx/fx}$) mice were crossed with *Tg (CAG-cre)13Miya*, which is a CAG-Cre ''transgenic general delete'' strain. Heterozygous mice ($Lgr4^{+/-}$) were then interbred to produce the null mice. The genetic backgrounds of the $Lgr4^{-/-}$ mice were C57BL/6Jx129Ola. $Lgr4^{+/-}$ female mice were housed with adult $Lgr4^{+/-}$ male mice overnight. The morning of the day of plugging was considered to be E0.5. In this study, $Lgr4^{+/+}$ was indicated a wild-type allele.

Lgr4 *Mutants and XY Genotyping of Mice*

The *Lgr4* mutant mouse lines and embryos were genotyped using methods reported previously. For sex chromosome typing, individual embryos were collected and DNA was isolated following routine methods. Y chromosome-specific sequences were detected by PCR using primers designed for the zinc finger protein, zinc finger protein 1, Y linked (*Zfy1*) (forward, 5′-GTAGGAAGAATCTTTCTCATGCTGG-3′; reverse, 5′-TTTTTGAGTGCT GATGGGTGACG-3′).

Histological and Immunohistochemical Analyses

All mice were killed and gonadal tissues were collected and imaged using a stereomicroscope (Leica MZ8; Leica Microsystems, Wetzlar, Germany). Urogenital ridges were fixed with 4% paraformaldehyde at 4°C overnight, dehydrated, embedded in paraffin, and then cut into 5-μm-thick sections. Immunological staining was performed using a rabbit polyclonal antibody against hydroxy-delta-5-steroid dehydrogenase, 3 beta- and steroid delta-isomerase cluster (HSD3B; dilution, 1:5000; University of Kyushu), a rabbit polyclonal antibody against SOX9 (dilution, 1:5000; University of Kyushu), a rabbit polyclonal antibody against LEF1 (dilution, 1:20; Cell Signaling Technology, Beverly, MA), a rabbit polyclonal antibody against DE-AD (Asp-Glu-Ala-Asp) box polypeptide 4 (DDX4; dilution, 1:1000; Novus Biologicals, LLC, Littleton, CO), an Alexa 594-labeled goat anti-mouse immunoglobulin (Ig) G antibody (dilution 1:1000; Invitrogen, Waltham, MA), and a peroxidase-labeled goat anti-rabbit IgG antibody (dilution, 1:1000; Vector Laboratories, Burlingame, CA). All tissue samples were viewed using an inverted microscope (Olympus IX70; Olympus America Inc., Hauppauge, NY). For frozen sections, samples were fixed in 4% paraformaldehyde for 20 min and then washed thrice in PBS for 10 min each. Samples were put through a sucrose gradient (15% and 30%), embedded in optimal cutting temperature compound, and cut into 5-μm-thick frozen sections. Immunofluorescence analysis was performed using the FluoView FV1200 Laser Scanning Microscope (Olympus). The immunological staining protocol used a rabbit polyclonal antibody against green fluorescent protein (GFP; dilution, 1:1000; Medical & Biological Laboratories, Co., Ltd., Nagoya, Japan), a goat polyclonal antibody against FOXL2 (dilution, 1:100; Abcam, Cambridge, UK), a mouse monoclonal antibody against keratin 8 (KRT8; dilution, 1:10; PRO-GEN, Heidelberg, Germany), an Alexa 488-labeled goat anti-mouse IgG antibody (dilution, 1:1000; Invitrogen), and Alexa 488-labeled goat anti-rabbit IgG antibody (dilution, 1:1000; Invitrogen). These antibodies were diluted with 5% normal goat serum in Tris-buffered saline or phosphate buffer and incubated overnight at 4°C for primary antibodies and 1 h at room temperature for secondary antibodies.

Cell Counts in Gonad Sections

Three sections were generated from each gonad sample. The numbers of FOXL2- and DDX4-positive cells were counted and compared between $Lgr4^{+/+}$ and $Lgr4^{-/-}$ mice. The number of cells in each section was counted per unit area (120×120 μm^2), and the average of these sections was considered a single data point. The total sample size (n) was 3–4.

Reverse Transcription-Polymerase Chain Reaction

Ovaries or testes from Postnatal Day (P) 0 (birth) pups ($Lgr4^{+/+}$ and $Lgr4^{-/-}$) were collected and the total RNA was isolated using TRIzol reagent (Invitrogen-Life Technologies). Complementary DNA was synthesized from 500 ng of total mRNA in 10 μl of the reaction mixture using the Premix Ex Taq (Perfect Real Time) Kit, according to the manufacturer's protocol (TaKaRa Bio, Inc., Otsu, Japan). PCR reactions were conducted using an initial incubation at 95°C for 2 min, followed by 30 cycles at 95°C for 30 sec, 64°C for 30 sec, and 72°C for 30 sec. The following primers were used: *Lgr4*-(F), 5′-CATTTTGGGGGTGTGACTCT-3′, *Lgr4*-(R), 5′-CGACCAGGAAAAT GAACCAC-3′; glyceraldehyde 3-phosphate dehydrogenase (*GAPDH)*-(F), 5′-CCAGAACATCATCCCTGCATC-3′, glyceraldehyde-3-phosphate dehydrogenase (*Gapdh)*-(R), 5′-CCTGCTTCACCACCTTCTTGA-3′; cytochrome P450, family 11, subfamily a, polypeptide 1 (*Cyp11a1*)-(F), 5′-GCTGGAA GGTGTAGCTCAGG-3′, *Cyp11a1*-(R), 5′-CACTGGTGTGGAACATCTGG-3′; hydroxysteroid (17-beta) dehydrogenase 3 (*Hsd17b3*)-(F), 5′-GTGTCATTCCCAGGCAGACC-3′, *Hsd17b3*-(R), 5′-GGTGAGGGGTGTC ATCTGAG-3′; cytochrome P450, family 17, subfamily a, polypeptide 1 (*Cyp17a1*)-(F), 5′-CTCTCTCCAGCCTGACAGAC-3′, *Cyp17a1*-(R), 5′-CTGGGTGTGGGTGTAATGAG-3′; and hydroxysteroid (17-beta) dehydrogenase 1 (*Hsd17b1*)-(F), 5′-CGATCCTGCTGCCGCTCTTT-3′, *Hsd17b1*-(R). *Gapdh* was used as an endogenous control.

Quantitative RT-PCR Analysis

Gonads of E14.5 mice were collected and the total RNA was isolated using TRIzol reagent. Complementary DNA was then synthesized from 100 ng of total mRNA in 20 μl of the reaction mixture using the Premix Ex Taq (Perfect Real Time) Kit, according to the manufacturer's protocol. Quantitative RT-PCR analysis was performed using the Thermal Cycler Dice Real Time System (TaKaRa Bio, Inc.) and SYBR Premix Ex Taq II Polymerase (TaKaRa Bio, Inc.) under the following conditions: 10 sec at 95°C followed by 40 cycles of 5 sec at 95°C and 30 sec at 60°C. Results are expressed as fold changes relative to the control using the ΔΔCt method. The values were standardized using ribosomal protein, large, P0 (*Rplp0*). The following primers were used: *Rplp0*-(F), 5′-ATAACCCTGAAGTGCTCGACAT-3′, *Rplp0*-(R), 5′-GGGAAGGTGTACTCAGTCTCCA-3′; *Lef1*-(F), 5′-TGAGTGCACGC TAAAGGAGA-3′, *Lef1*-(R), 5′-GCTGTCATTCTGGGACCTGT-3′; *Axin2*-(F), 5′-CAGGAGGATGCTGAAGGCTCAAAGC-3′, and *Axin2*-(R), 5′-CTCAAAAACTGCTCCGCAGGCAAAT-3′, *trans*-acting transcription factor 5 (*Sp5*)-(F), 5′-TGGGTTCACCCTCCAGACTTT-3′, and *Sp5*-(R), 5′-CCGGCGAGAACTCGTAAGG-3′.

Differentiation of the Estrus Cycle

Differentiation of the estrus cycle has been previously described [29]. Vaginal epithelial cells from wild-type, sexually mature, female mice were smeared on a slide glass using a swab and then stained using Giemsa's azur-eosin-methylene blue solution (Merck KGaA, Darmstadt, Germany) for 30 sec and rinsed with tap water. According to the morphology of epithelial cells and leukocytes viewed under a microscope, the estrus cycle was classified into four phases: 1) proestrus phase (P phase), characterized by nucleated epithelial cells;

2) metestrus phase (M phase), characterized by anucleated cornified epithelial cells and leukocytes; 3) estrous phase (E phase), characterized by anucleated cornified epithelial cells; and 4) diestrus phase (D phase), characterized by nucleated epithelial cells.

Superovulation Process

Female wild-type mice (age, 25–30 wk) were used to investigate the superovulation process. Equine chorionic gonadotropin (eCG; PEAMEX; Yell Pharmaceutical Co., Ltd., Tokyo, Japan) was dissolved in PBS and 15 IU was intraperitoneally injected into each mouse. Human chorionic gonadotropin (hCG; PUBEROGEN; Yell Pharmaceutical Co., Ltd.) was dissolved in PBS. Each mouse was injected with 15 IU of hCG 48 h after eCG administration. Single injections of eCG were administered as stated above (15 IU/mouse, intraperitoneal injection).

Testosterone and Androstenedione Measurement Using Liquid Chromatography-Tandem Mass Spectrometry

The steroid measurement has been previously described [30]. Ovaries and testes of P0 pups were collected in 5-ml polypropylene tubes and quickly stored at −80°C for future use. Prior to homogenization, ethyl acetate (300 ml) was added to the frozen samples, which were then subjected to three freeze/thaw cycles. The deuterium-labeled internal standards (testosterone-d3 and androstenedione-d7) were subsequently added to each tube. Samples were homogenized at room temperature for 1 min using a Polytron PT1200E Homogenizer (Kinematica AG, Lucerne, Switzerland) at the highest setting. The homogenizer shaft was washed with ethyl acetate (300 ml) and the samples were returned to the original tubes. The homogenates were centrifuged at 3800 $\times$ *g* for 10 min to separate insoluble debris, and the supernatant (ethyl acetate) was transferred to a fresh 2.0-ml microcentrifuge tube. Each step of this protocol was repeated twice (total volume, 1.2 ml). The solution was evaporated using a CVE-3100 Vacuum Centrifuge (Tokyo Rikakikai Co., Ltd., Tokyo, Japan) with a UT-1000 Cold Trap (Tokyo Rikakikai Co., Ltd.). Liquid chromatography (LC) was performed using an Ultimate 3000 HPLC System (Dionex Corp., Sunnyvale, CA) with a ZORBAX Eclipse XDB-C18 Column (150 $\times$ 2.1 mm inside diameter; 3.5 mm; 80 A; Agilent Technologies Inc., Santa Clara, CA). Tandem mass spectrometry (MS/MS) was performed using a TSQ Vantage Triple-Stage Quadrupole Mass Spectrometer (Thermo Fisher Scientific Inc., Waltham, MA) with an electrospray ionization source in positive ion mode. Standard curves were constructed based on LC-MS/MS analysis of a mixture including each target androgen with the corresponding internal standard (testosterone-d3 and androstenedione-d7).

Statistical Analysis

All values are expressed as the means ± SEM unless indicated otherwise. Differences between mean values among groups were determined by *t*-tests using GraphPad software (GraphPad Software Inc., La Jolla, CA) and the statistical analysis function of Microsoft Excel (2007 version; Microsoft Corp., Redmond, WA). A probability (*P*) value of less than 0.05 was considered statistically significant.

RESULTS

Lgr4 *Is Expressed in Female Somatic Cells of the Ovaries During the Embryonic and Neonatal Periods*

We investigated the LGR4 expression pattern in the gonads during the embryonic period (Fig. 1). $Lgr4^{EGFP\text{-}IRES\text{-}CreERT2/+}$ mice at E14.5 were subjected to immunohistological analysis with anti-GFP antibodies. EGFP was expressed in the gonads, but not in the mesonephros, including the Wolffian and Müllerian ducts in female $Lgr4^{EGFP\text{-}IRES\text{-}CreERT2/+}$ mice at E14.5 (Fig. 1, A–D). To investigate the types of cells that expressed EGFP, we performed double immunostaining using anti-GFP with anti-FOXL2 (a marker of pregranulosa cells), anti-Keratin8 (a marker of the coelomic epithelium), or anti-DDX4 (a marker of germ cells) (Fig. 1, E–G). Almost all FOXL2-positive cells were also labeled with GFP, while GFP-positive but FOXL2-negative cells were more broadly distributed in gonads than were cells expressing only FOXL2 (Fig. 1E). Some KRT8-positive cells were colocalized with GFP-positive cells (Fig. 1F). These data suggest that that LGR4 was expressed broadly in somatic cells, including FOXL2-positive cells and coelomic epithelial cells (KRT8-positive cells). However, LGR4 was detected more strongly in the medullary region than in the cortex in gonads. No cells expressed both EGFP and DDX4, suggesting that LGR4 was not expressed in germ cells (Fig. 1G).

Lgr4$^{-/-}$ *Female Mice Are Characterized by Impaired Urinary and Reproductive Organs*

The $Lgr4^{-/-}$ phenotype is lethal during neonatal stages. Therefore, to determine the phenotype of the gonads and reproductive tissues of $Lgr4^{-/-}$ females, we performed hematoxylin and eosin staining at E14.5 and P0, and observed the gross morphology at P0 (Fig. 2). At E14.5, no typical differences were observed between the gonadal structure of $Lgr4^{+/+}$ and $Lgr4^{-/-}$ females (Fig. 2, A–C). Both the Wolffian and Müllerian ducts were present in $Lgr4^{-/-}$ females, indicating that *Lgr4* defects did not cause Müllerian duct deficiency, which is observed in $Wnt4^{-/-}$ mice [27]. However, we found that $Lgr4^{-/-}$ females developed male-like blood vessels (Fig. 2, D–F). In $Lgr4^{-/-}$ females at P0, coiled ductal structures resembling the male epididymis were observed around the gonads (Fig. 2, I and N). Furthermore, vas deferens-like ducts were parallel to the normal uterine horn (Fig. 2, J and Q). These phenotypes, with ectopic ductal structures and male-like blood vessels, resembled those of $Rspo1^{-/-}$ females, which harbor both female and male ducts [28, 31].

Abnormal Expression of Sex Steroid Synthetic Enzymes in Lgr4$^{-/-}$ *Gonads*

Previous analyses revealed ectopic steroidogenic cells in female $Rspo1^{-/-}$ gonads, suggesting that these cells produce male hormones to stimulate male-like ductal development [28, 31]. We investigated whether masculinization and development of male-like ducts in $Lgr4^{-/-}$ females also occurred in response to unusual steroidogenic cells of gonads during the embryonic period. We performed immunohistochemical analysis of HSD3B, a steroidogenic enzyme involved in testosterone production (Fig. 3). We observed HSD3B-positive cells in the stromal cells of the E14.5 $Lgr4^{+/+}$ testes (Fig. 3, G–I). Furthermore, we identified HSD3B-positive cells scattered throughout the $Lgr4^{-/-}$ ovaries of E16.5 mice, but not the E14.5 $Lgr4^{-/-}$ ovaries (Fig. 3, D–F). In $Lgr4^{+/+}$ ovaries, we detected weak staining of HSD3B from E14.5 to P0. However, this staining was significantly weaker than staining in the $Lgr4^{-/-}$ ovary, which was closer in intensity to that observed in $Lgr4^{+/+}$ male mice (Fig. 3, A–C). We investigated whether P0 $Lgr4^{-/-}$ ovaries produced androgen synthetic enzymes by RT-PCR (Fig. 3J). We investigated *Cyp11a1*, *Hsd3b*, *Cyp17a1*, *Hsd17b1*, and *Hsd17b3* genes. Expression of the sex hormone synthetic enzyme genes was not observed in $Lgr4^{+/+}$ females, in contrast to $Lgr4^{-/-}$ females. The expression pattern of sex hormone synthetic enzymes in $Lgr4^{-/-}$ females was similar to that of $Lgr4^{+/+}$ males.

We investigated androgen production in the ovaries of $Lgr4^{-/-}$ females by measuring their levels in the gonads of P0 mice using LC-MS/MS (Supplemental Figure S1, available online at www.biolreprod.org). We suspected two potential causes of male specialization of female embryonic gonads. Accordingly, we measured testosterone and androstenedione levels. Based on our results, there were no significant differences in testosterone and androstenedione levels between $Lgr4^{+/+}$ and $Lgr4^{-/-}$ females.

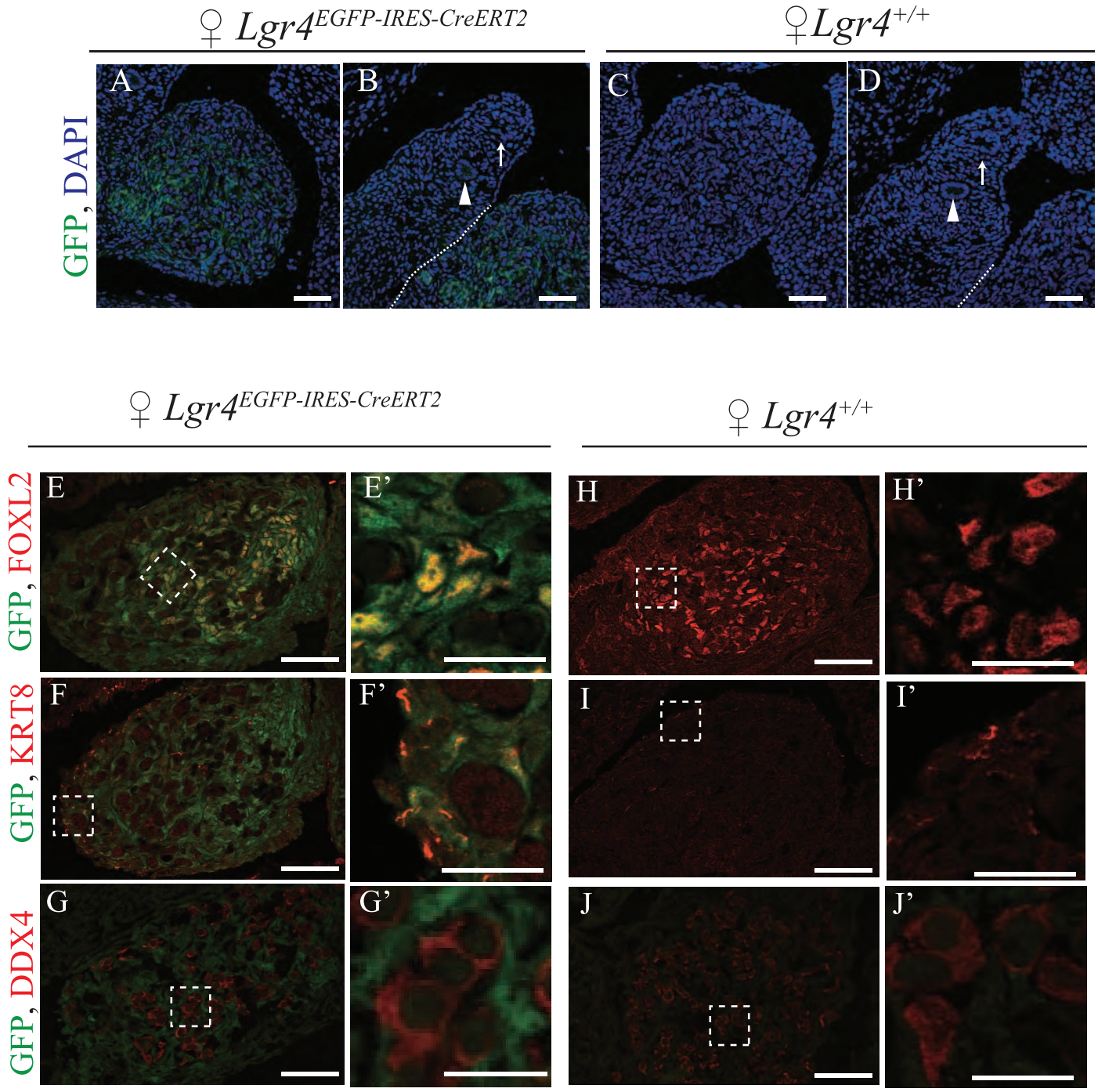

FIG. 1. *Lgr4* expression in ovaries at 14.5. **A**–**D**) Immunohistorogical staining for GFP were performed with $Lgr4^{EGFP\text{-}IRES\text{-}CreERT2/+}$ female (**A** and **B**) and $Lgr4^{+/+}$ female (**C** and **D**) at E14.5. The image of the gonadal area is shown in **A** and **C**. The image of the mesonephros area is shown in **B** and **D**. White arrowheads, Wolffian duct; white arrows, Müllerian duct; white dotted line, border between gonad and mesonephros. Bars = 50 μm. Nucleus was stained with DAPI. **E**–**J**) Double immunohistological staining for GFP and FOXL2, KRT8, or DDX4 was performed with $Lgr4^{EGFP\text{-}IRES\text{-}CreERT2/+}$ (**E**–**G**) and $Lgr4^{+/+}$ (**H**–**J**) females at E14.5. Bars = 50 μm. The regions outlined by the white boxed areas in **E**–**J** are shown at higher magnification in **E'**–**J'**, respectively. Bars = 20 μm.

FIG. 2. Morphological observation of the reproductive tracts in $Lgr4^{+/+}$ female, $Lgr4^{-/-}$ female, and $Lgr4^{+/+}$ male. **A**–**C**) Hematoxylin and eosin (HE)-stained section from the reproductive tracts of $Lgr4^{+/+}$ female (**A**), $Lgr4^{-/-}$ female (**B**), and $Lgr4^{+/+}$ male (**C**) at E14.5. Black arrowheads, Wolffian duct; black arrows, Müllerian duct. Bars = 100 μm. **D**–**F**) The coelomic vessel of $Lgr4^{-/-}$ female at E14.5 using the stereomicroscope: $Lgr4^{+/+}$ female (**D**), $Lgr4^{-/-}$ female (**E**), and $Lgr4^{+/+}$ male (**F**). Black dotted line, gonads; black arrows, coelomic vessels of gonads. Bar = 1 mm. **G**–**K**) Gross morphology of the

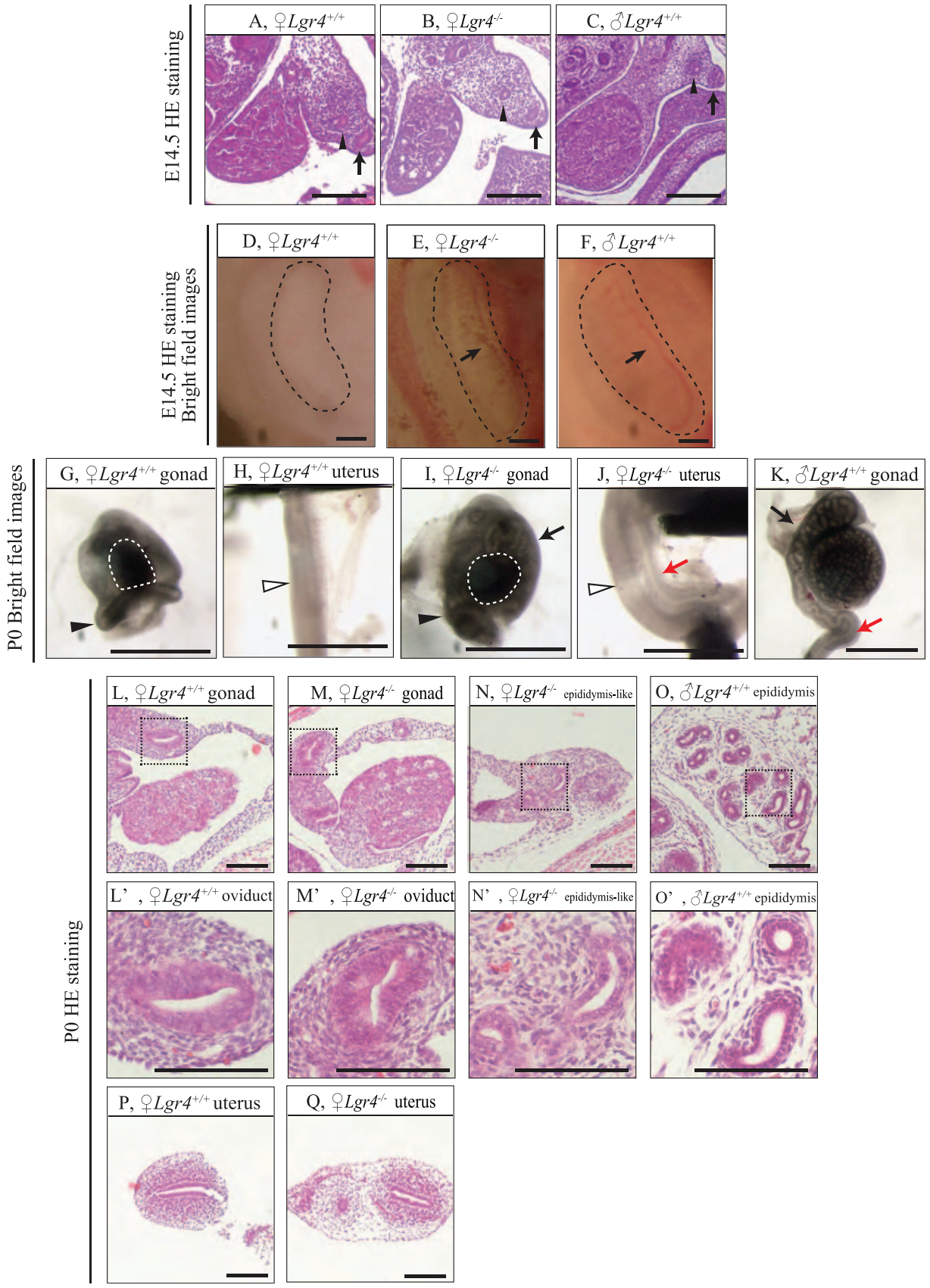

reproductive tracts in *Lgr4*$^{+/+}$ female (**G** and **H**), *Lgr4*$^{-/-}$ female (**I** and **J**), and *Lgr4*$^{+/+}$ male (**K**) at P0. Black arrowheads, oviduct; black arrows, epididymis in male or epididymis-like structure in *Lgr4*$^{-/-}$ female; red arrows, vas deference in male or vas deference-like structure in *Lgr4*$^{-/-}$ female; white arrowheads, uterus; white dotted line, ovaries. Bars = 1 mm. **L**–**Q**) HE-stained section from the reproductive tracts of in *Lgr4*$^{+/+}$ female (**L**, **L'**, and **Q**), *Lgr4*$^{-/-}$ female (**M**, **M'**, **N**, **N'**, and **Q**), and *Lgr4*$^{+/+}$ male (**O** and **O'**) at P0. The regions outlined by the black boxed areas in **L**–**O** are shown at higher magnification in **L'**–**O'**, respectively. Bars = 100 μm.

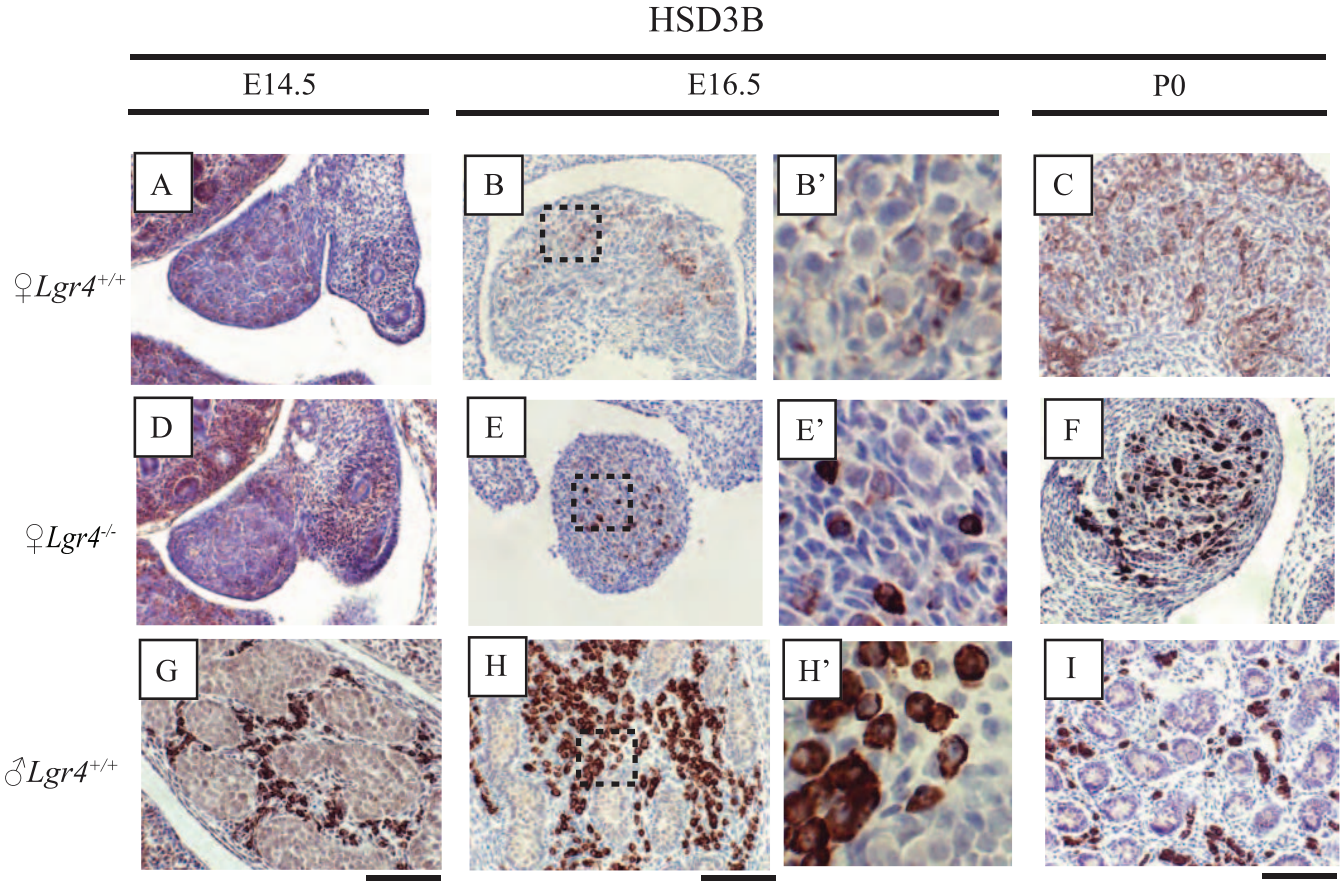

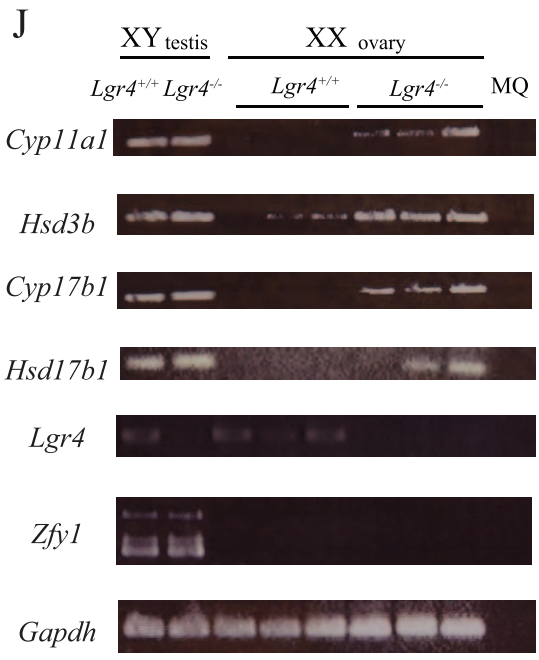

FIG. 3. The expression of sex steroid synthetic enzyme in ovaries and testes at E14.5, E16.5, and P0. **A–I**) Immunohistological staining for HSD3B was performed with *Lgr4*$^{+/+}$ female (**A–C**), *Lgr4*$^{-/-}$ female (**D–F**), and *Lgr4*$^{+/+}$ male (**G–I**) at E14.5 (**A**, **D**, **G**), E16.5 (**B**, **B'**, **E**, **E'**, **H**, **H'**) and P0 (**C**, **F**, **I**). The regions outlined by the black boxed areas in **B**, **E**, and **H** are shown at higher magnification in **B'**, **E'**, and **H'**, respectively. Bars = 100 μm. **J**) RT-PCR analysis was performed with gonad samples of *Lgr4*$^{+/+}$ male, *Lgr4*$^{+/+}$ and *Lgr4*$^{-/-}$ female, and *Lgr4*$^{-/-}$ female at P0. Three independent tissue samples were used for electrophoresis in females. We used primer pairs to detect transcripts for sex steroidogenic enzyme genes (*Cyp11a1*, *Hsd3b*, *Cyp17a1*, and *Hsd17b1*), *Lgr4*, *Zfy1*, and *Gapdh*. *Gapdh* was used as an endogenous control. Milli Q (MQ) water was the negative control.

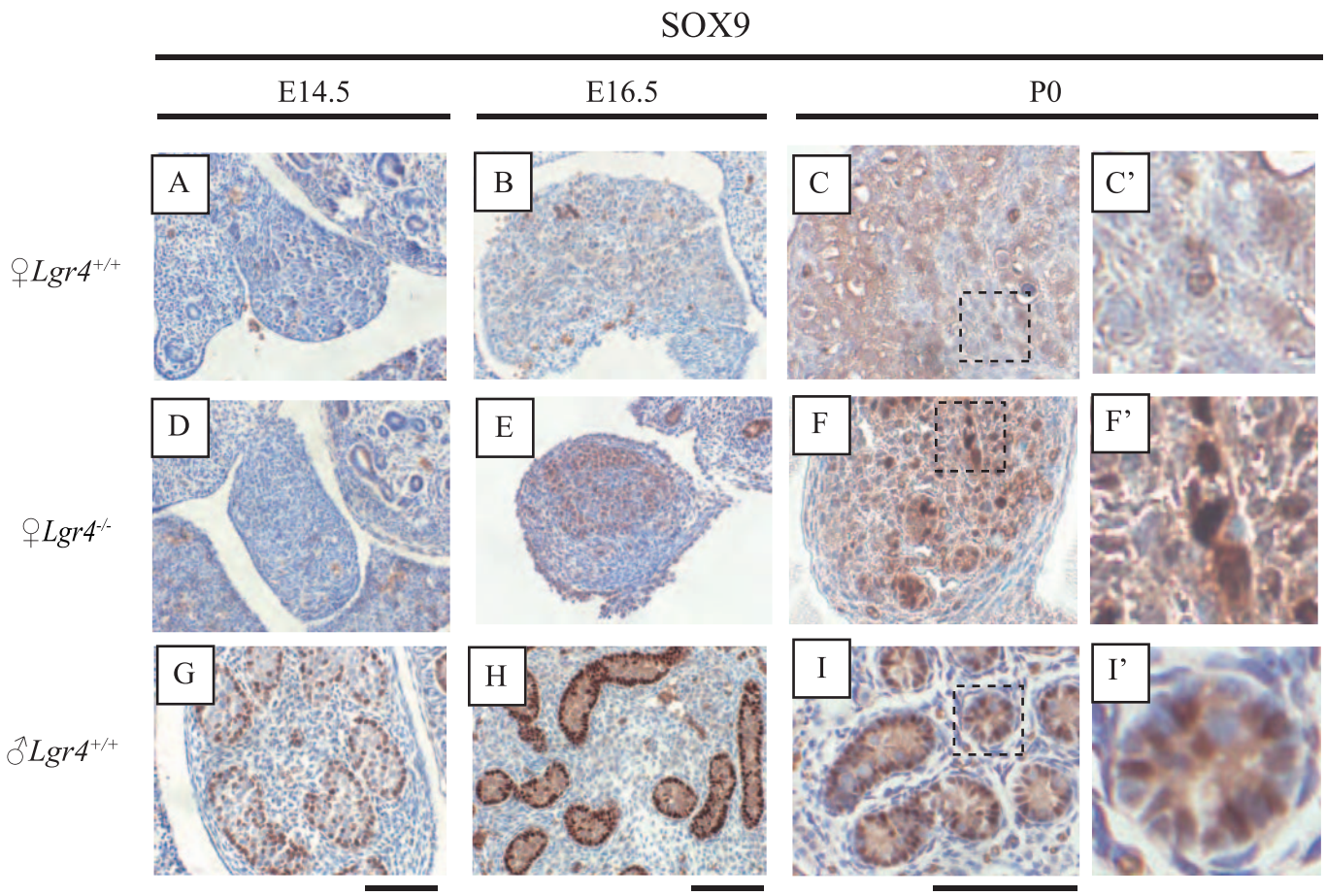

FIG. 4. SOX9 expression in ovaries and testes at E14.5, E16.5, and P0. **A**–**C**) Testes of *Lgr4*$^{+/+}$ female mice. **D**–**F**) Ovaries of *Lgr4*$^{-/-}$ female mice. **G**–**I**) Ovaries of *Lgr4*$^{+/+}$ male mice. The regions outlined by the black boxed areas in **C**, **F**, and **I** are shown at higher magnification in **C′**, **F′**, and **I′**, respectively. **A**, **D**, and **G** at E14.5; **B**, **E**, and **H** at E16.5; and **C**, **C′**, **F**, **F′**, **I**, and **I′** at P0. Bars = 100 μm.

Ectopic Expression of Sox9 *in* Lgr4$^{-/-}$ *Gonads*

Loss-of-function mutations in *Rspo1* and *Wnt4* in mice lead to ectopic expression of male gonadal-specific genes, such as *Sox9* [28, 31]. At E14.5, E16.5, and P0, SOX9-positive cells were observed on the basement membrane side of the *Lgr4*$^{+/+}$ testis (Fig. 4, G–I). In *Lgr4*$^{-/-}$ ovaries, we did not find a clear indication of Sox9-positive cells at E14.5 (Fig. 4D). SOX9-positive cells were lightly distributed throughout E16.5 and P0 *Lgr4*$^{-/-}$ ovaries (Fig. 4, E and F). Although weak SOX9 staining was observed in the *Lgr4*$^{+/+}$ ovaries, it was diffuse and not nuclear (Fig. 4, A–C).

FOXL2-Positive Pregranulosa Cells and Germ Cells Were Decreased in Lgr4$^{-/-}$ *Gonads*

As shown in Figure 1, LGR4-EGFP-positive cells were colocalized with FOXL2, which is expressed in pregranulosa cells and regulates sex determination [22, 32]. We detected FOXL2 expression by immunohistochemical analysis using E14.5 *Lgr4*$^{+/+}$ and *Lgr4*$^{-/-}$ mice, and we counted the number of FOXL2-positive cells. We found significantly fewer FOXL2-positive cells in *Lgr4*$^{-/-}$ mice than in *Lgr4*$^{+/+}$ mice at E14.5 (Fig. 5, A–C). These results suggest that *Lgr4* defects caused the abnormal phenotypes similar to those observed in *Wnt4*$^{-/-}$ and *Rspo1*$^{-/-}$ female gonads, strongly suggesting that LGR4 acts as an RSPO1 receptor in the sex determination pathway during female gonadal development.

In female *Rspo1*$^{-/-}$ gonads, the number of germ cells was reduced and germ cells resembled G0–G1 arrested gonocytes, like male germ cells [26]. We performed immunohistochemical analysis against DDX4 with E14.5 samples. The number of DDX4-positive cells was significantly lower in *Lgr4*$^{-/-}$ than in *Lgr4*$^{+/+}$ mice (Fig. 5, D–F). This decreased number of germ cells in *Lgr4*$^{-/-}$ gonads was similar to that of *RSPO1*$^{-/-}$ mice.

Wnt/Beta-Catenin Signaling Is Decreased in Lgr4$^{-/-}$ *Ovaries*

The phenotypes of female *Lgr4*$^{-/-}$ gonads were similar to those of *Rspo1*$^{-/-}$ gonads, suggesting that specialization of female gonad somatic cells was regulated by Wnt/beta-catenin signaling via RSPO1/LGR4. The expression levels of the target genes of Wnt/beta-catenin signaling, such as *Lef1* and *Axin2*, were decreased in *RSPO1*$^{-/-}$ gonads [26]. Immunohistochemical staining of LEF1, which is a target gene of Wnt signaling, was performed using E14.5 gonads (Fig. 6). In female *Lgr4*$^{-/-}$ gonads, the LEF1 signal was lower than it was in *Lgr4*$^{+/+}$ gonads in the medullary region (Fig. 6, A and B). However, LEF1 expression was not decreased in the coelomic epithelium. Based on quantitative RT-PCR (qRT-PCR) results, *Axin2* expression in *Lgr4*$^{-/-}$ gonads was significantly lower than it was in *Lgr4*$^{+/+}$ gonads. Although not statistically significant, we found that *Lgr4*$^{-/-}$ ovaries tended to have decreased

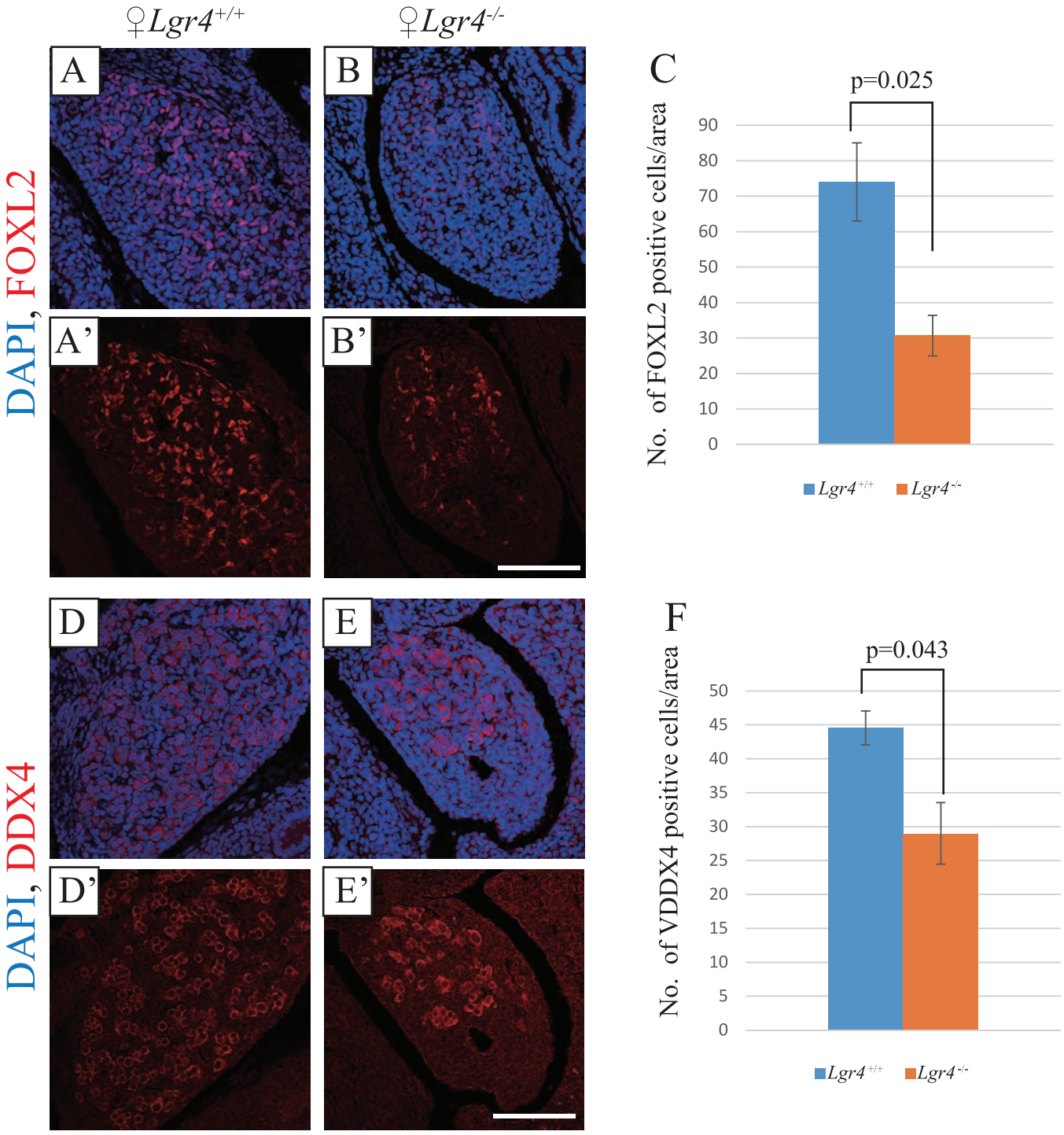

FIG. 5. The numbers of FOXL2-positive cells and germ cells were decreased in *Lgr4*$^{-/-}$ female mice. **A**, **B**, **D**, and **E**) Immunostaining for FOXL2 (**A** and **B**) or DDX4 (**D** and **E**) was performed at E14.5. **A** and **D**) *Lgr4*$^{-/-}$ ovary. **B** and **E**) *Lgr4*$^{+/+}$ ovary. **C** and **F**) The number of FOXL2- or DDX4-positive cells per area (120 × 120 μm^2) were counted and compared between *Lgr4*$^{+/+}$ and *Lgr4*$^{-/-}$ (n = 3–4). Nuclei were stained with DAPI. **A′**, **B′**, **D′**, and **E′**) Immunostaining for FOXL2 (**A′** and **B′**) or DDX4 (**D′** and **E′**) without DAPI. Bars = 100 μm. Error bars, mean ± SEM.

expression of *Lef1* and *Sp5* (another target gene of Wnt/beta-catenin signaling; Fig. 6C).

Lgr4 *Was Expressed in Adult Ovaries*

Lgr4$^{-/-}$ mice are neonatal lethal. To analyze the function of LGR4 in adult female mice, we analyzed *Lgr4* expression in the adult ovary during each phase of the estrus cycle using qRT-PCR (Fig. 7). *Lgr4* expression increased with the onset of ovulation during estrus. When ovarian hyperstimulation was induced by injection of eCG and hCG, we detected a remarkable upregulation of *Lgr4* expression at 16 h (when ovulation was most active). We thought that *Lgr4* might participate in ovum maturity, ovulation, and luteal function in mature mice. To analyze the function of LGR4 in adult mice, we used conditional KOs with Amhr-Cre mice to avoid lethality. The results of this analysis revealed no abnormalities

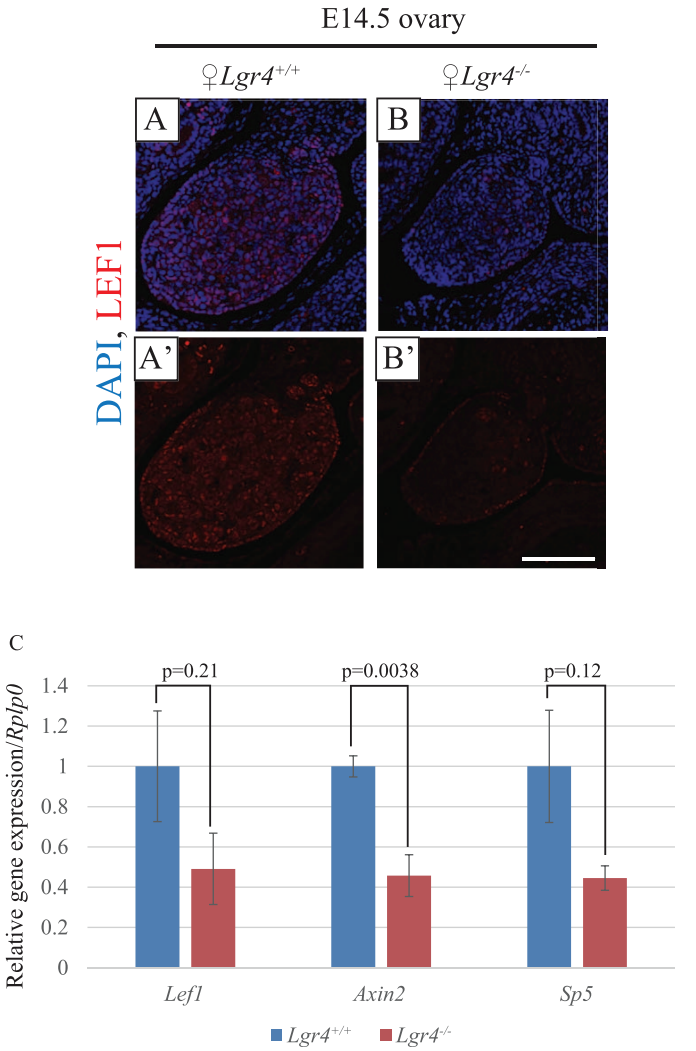

FIG. 6. The expression of Wnt/beta-catenin signaling-related genes in *Lgr4*$^{-/-}$ ovary. Immunostaining for LEF1 was performed at E14.5. **A**) *Lgr4*$^{+/+}$ ovary. **B**) *Lgr4*$^{-/-}$ ovary. Nuclei were stained with DAPI. **A′** and **B′**) Immunostaining for LEF1 without DAPI. Bars = 100 μm. **C**) Quantitative RT-PCR for *Lef1 Axin2*, *Sp5* expression in *Lgr4*$^{+/+}$ or *Lgr4*$^{-/-}$ ovaries at E14.5 (n = 3–4). Error bars, mean ± SEM.

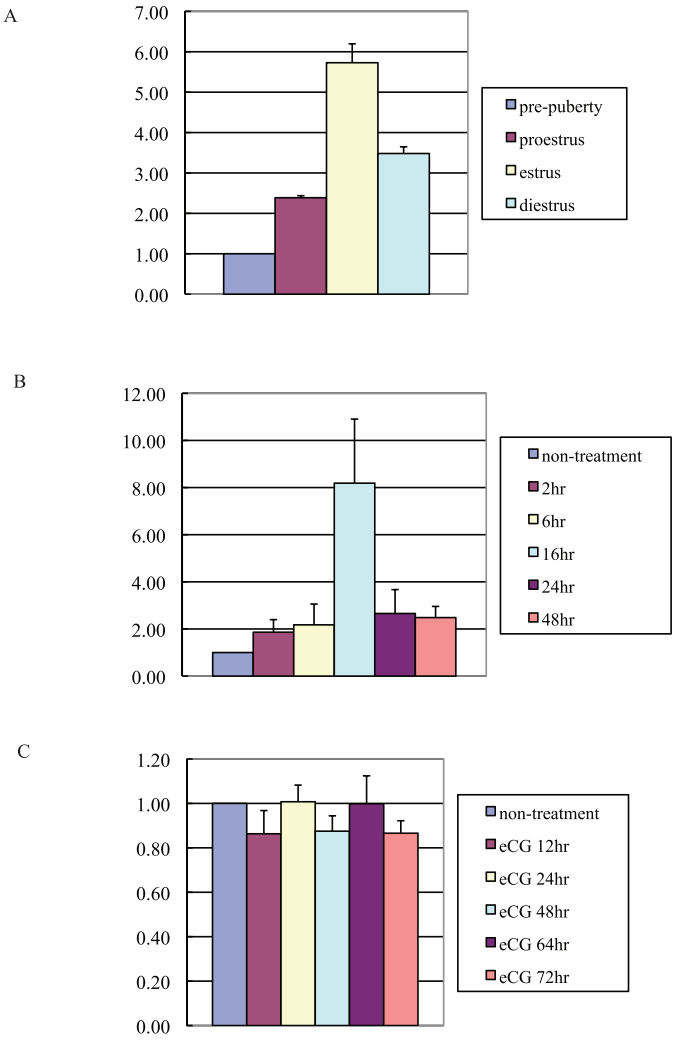

FIG. 7. Quantitative RT-PCR for *Lgr4* ovarian expression in each estrus cycle and when ovarian hyperstimulation was induced by injections of eCG and hCG. **A**) The expression of *Lgr4* gene along the ovulatory cycle; qRT-PCR was performed for RNA from ovaries. **B**) Quantitative RT-PCR for *Lgr4* ovarian expression after the treatment of the superovulation at 6, 16, and 24 h after administration of hCG. **C**) Quantitative RT-PCR for *Lgr4* ovarian expression after treatment of only eCG.

in the phenotype, ovulation cycle, or female fertility (data not shown).

DISCUSSION

We investigated the function of LGR4 in the reproductive organs of mice. The *Lgr4*$^{-/-}$ genotype is lethal during neonatal stages [16]. Therefore, we initially analyzed neonatal mice and found that *Lgr4*$^{-/-}$ females had vestigial remnants of Wolffian ducts. *Lgr4*$^{-/-}$ females had male epididymis-like ducts surrounding their gonads, and vas deferens-like ducts along the uteri. These phenotypes are commonly observed in *Rspo1*$^{-/-}$ female mice [28, 31]. Similar to that observed in *Rspo1*$^{-/-}$ female mice, the expression of steroidogenic enzyme genes, such as *Hsd17b3*, *Hsd3b*, *Cyp17a1*, and *Cyp11a1* were strongly upregulated in the *Lgr4*$^{-/-}$ female gonads at P0. It is likely that these steroidogenic cells produce hormones to stimulate the development of the epididymis and vas deferens in *Lgr4*$^{-/-}$ females.

Wolffian and Müllerian ducts formed normally in the *Lgr4*$^{-/-}$ female mesonephros at E14.5, unlike that observed in *Wnt4*$^{-/-}$ mice [27]. In this study, we found that *Lgr4*-EGFP was expressed in the gonads, but not in the mesonephros, and *Rspo1* is known to show a similar expression pattern [25]. However, *Wnt4* is expressed throughout the mesonephros [27, 33]. The phenotypic differences between *Rspo1*$^{-/-}$, *Lgr4*$^{-/-}$, and *Wnt4*$^{-/-}$ mice might reflect differences in the expression patterns of these genes.

Recently, cooperative signaling of RSPOs and Wnt has been reported; this signaling may be related to gonadal development in mice. We suspected that LGR4-mediated Wnt/beta-catenin signaling regulates somatic cell differentiation in mouse embryonic ovaries. We observed that Wnt targets, such as *Lef1* and *Axin2*, were downregulated in *Lgr4*$^{-/-}$ female ovaries. LEF1 expression was reduced in somatic cells in the medullary region, but not in the coelomic epithelium. In *Lgr4*-EGFP mice, LGR4 was detected more strongly in the medullary region than in the cortex, suggesting

that LGR4 might be important for the regulation of Wnt/beta-catenin signaling in precursors of ovarian somatic cells in the medial region, such as in FOXL2-expressing cells. However, *Lgr5*, a marker of granulosa precursor cells, has been shown to be expressed in the cortical region. These data suggest that RSPO1 promotes Wnt/beta-catenin signaling in somatic cells via LGR4 in the medullary region, but via LGR5 in the cortical region [34, 35].

To examine the function of LGR4 in the adult ovary, we used conditional KO Amhr-Cre mice. However, the result of this analysis revealed no abnormalities in the phenotype, ovulation cycle, or female fertility. Pan et al. reported the requirement of *Lgr4* for steroid production in granulosa-lutein cells during luteinization [36]. They analyzed the function of *Lgr4* during the adult stage using the *Lgr4* gene-trap mouse strain, which contains all *Lgr4* coding exons, and about half escaped perinatal lethality. Our $Lgr4^{-/-}$ mice showed complete deletion of the *Lgr4* exon 18 region, which accounts for the whole transmembrane coding domain, using the loxP site knockin strategy, and they all died within 2 days of birth, suggesting a more severe phenotype than that of the Yi et al. mouse line. Therefore, we focused on the embryonic and prenatal stages, and identified the impairment of female gonadal development caused by the complete deletion of *Lgr4*. Therefore, LGR4 has essential functions in the developmental of fetal female gonads and a potential relation to the ovulatory cycle in adult stages.

ACKNOWLEDGMENT

We are grateful to Drs. Kanako Miyabayashi and Kenichiro Morohashi for kindly providing the anti-HSD3B antibody and anti-SOX9 antibody.

REFERENCES

1. Van Loy T, Vandersmissen HP, Van Hiel MB, Poels J, Verlinden H, Badisco L, Vassart G, Vanden Broeck J. Comparative genomics of leucine-rich repeats containing G protein-coupled receptors and their ligands. Gen Comp Endocrinol 2008; 155:14–21.
2. Kohn LD, Shimura H, Shimura Y, Hidaka A, Giuliani C, Napolitano G, Ohmori M, Laglia G, Saji M. The thyrotropin receptor. Vitam Horm 1995; 50:287–384.
3. Ji TH, Ryu KS, Gilchrist R, Ji I. Interaction, signal generation, signal divergence, and signal transduction of LH/CG and the receptor. Recent Prog Horm Res 1997; 52:431–453; discussion 454.
4. Simoni M, Gromoll J, Nieschlag E. The follicle-stimulating hormone receptor: biochemistry, molecular biology, physiology, and pathophysiology. Endocr Rev 1997; 18:739–773.
5. Dufau ML. The luteinizing hormone receptor. Annu Rev Physiol 1998; 60:461–496.
6. Hsu SY, Kudo M, Chen T, Nakabayashi K, Bhalla A, van der Spek PJ, van Duin M, Hsueh AJ. The three subfamilies of leucine-rich repeat-containing G protein-coupled receptors (LGR): identification of LGR6 and LGR7 and the signaling mechanism for LGR7. Mol Endocrinol 2000; 14: 1257–1271.
7. Park JI, Semyonov J, Chang CL, Hsu SY. Conservation of the heterodimeric glycoprotein hormone subunit family proteins and the LGR signaling system from nematodes to humans. Endocrine 2005; 26: 267–276.
8. Vodstrcil LA, Wlodek ME, Parry LJ. Effects of uteroplacental restriction on the relaxin-family receptors, Lgr7 and Lgr8, in the uterus of late pregnant rats. Reprod Fertil Dev 2007; 19:530–538.
9. Barker N, Tan S, Clevers H. Lgr proteins in epithelial stem cell biology. Development 2013; 140(12):2484–2494.
10. Kato S, Mohri Y, Matsuo T, Ogawa E, Umezawa A, Okuyama R, Nishimori K. Eye-open at birth phenotype with reduced keratinocyte motility in LGR4 null mice. FEBS Lett 2007; 581:4685–4690.
11. Mohri Y, Umezu T, Hidema S, Tomisawa H, Akamatsu A, Kato S, Nawa A, Nishimori K. Reduced fertility with impairment of early-stage embryos observed in mice lacking Lgr4 in epithelial tissues. Fertil Steril 2010; 94: 2878–2881.
12. Sone M, Oyama K, Mohri Y, Hayashi R, Clevers H, Nishimori K. LGR4 expressed in uterine epithelium is necessary for uterine gland development and contributes to decidualization in mice. FASEB J 2013; 27:4917–4928.
13. Carmon KS, Gong X, Lin Q, Thomas A, Liu Q. R-spondins function as ligands of the orphan receptors LGR4 and LGR5 to regulate Wnt/beta-catenin signaling. Proc Natl Acad Sci U S A 2011; 108:11452–11457.
14. de Lau W, Barker N, Low TY, Koo BK, Li VS, Teunissen H, Kujala P, Haegebarth A, Peters PJ, van de Wetering M, Stange DE, van Es JE, et al. Lgr5 homologues associate with Wnt receptors and mediate R-spondin signalling. Nature 2011; 476:293–297.
15. Glinka A, Dolde C, Kirsch N, Huang YL, Kazanskaya O, Ingelfinger D, Boutros M, Cruciat CM, Niehrs C. LGR4 and LGR5 are R-spondin receptors mediating Wnt/beta-catenin and Wnt/PCP signalling. EMBO Rep 2011; 12:1055–1061.
16. Kato S, Matsubara M, Matsuo T, Mohri Y, Kazama I, Hatano R, Umezawa A, Nishimori K. Leucine-rich repeat-containing G protein-coupled receptor-4 (LGR4, Gpr48) is essential for renal development in mice. Nephron Exp Nephrol 2006; 104:e63–e75.
17. Jost A. Hormonal factors in the sex differentiation of the mammalian foetus. Philos Trans R Soc Lond B Biol Sci 1970; 259:119–130.
18. Sekido R, Lovell-Badge R. Sex determination and SRY: down to a wink and a nudge? Trends Genet 2009; 25:19–29.
19. MacLaughlin DT, Donahoe PK. Sex determination and differentiation. New Engl J Med 2004; 350:367–378.
20. Berta P, Hawkins JR, Sinclair AH, Taylor A, Griffiths BL, Goodfellow PN, Fellous M. Genetic evidence equating SRY and the testis-determining factor. Nature 1990; 348:448–450.
21. Crisponi L, Deiana M, Loi A, Chiappe F, Uda M, Amati P, Bisceglia L, Zelante L, Nagaraja R, Porcu S, Serafina Ristaldi M, Marzella R, et al. The putative forkhead transcription factor FOXL2 is mutated in blepharophimosis/ptosis/epicanthus inversus syndrome. Nat Genet 2001; 27:159–166.
22. Schmidt D, Ovitt CE, Anlag K, Fehsenfeld S, Gredsted L, Treier AC, Treier M. The murine winged-helix transcription factor Foxl2 is required for granulosa cell differentiation and ovary maintenance. Development 2004; 131:933–942.
23. Uhlenhaut NH, Jakob S, Anlag K, Eisenberger T, Sekido R, Kress J, Treier AC, Klugmann C, Klasen C, Holter NI, Riethmacher D, Schutz G, et al. Somatic sex reprogramming of adult ovaries to testes by FOXL2 ablation. Cell 2009; 139:1130–1142.
24. Chassot AA, Gillot I, Chaboissier MC. R-spondin1, WNT4, and the CTNNB1 signaling pathway: strict control over ovarian differentiation. Reproduction 2014; 148:R97–110.
25. Parma P, Radi O, Vidal V, Chaboissier MC, Dellambra E, Valentini S, Guerra L, Schedl A, Camerino G. R-spondin1 is essential in sex determination, skin differentiation and malignancy. Nat Genet 2006; 38: 1304–1309.
26. Chassot AA, Gregoire EP, Lavery R, Taketo MM, de Rooij DG, Adams IR, Chaboissier MC. RSPO1/beta-catenin signaling pathway regulates oogonia differentiation and entry into meiosis in the mouse fetal ovary. PLoS One 2011; 6:e25641.
27. Vainio S, Heikkila M, Kispert A, Chin N, McMahon AP. Female development in mammals is regulated by Wnt-4 signalling. Nature 1999; 397:405–409.
28. Chassot AA, Ranc F, Gregoire EP, Roepers-Gajadien HL, Taketo MM, Camerino G, de Rooij DG, Schedl A, Chaboissier MC. Activation of beta-catenin signaling by Rspo1 controls differentiation of the mammalian ovary. Hum Mol Genet 2008; 17:1264–1277.
29. Tanaka Y. Histochemical change of the vaginal smear, epithelium and the endometrium of the mouse during the sex cycle [article in Japanese]. J Jpn Obstet Gynecol Soc 1962; 14:273–282.
30. McNamara KM, Harwood DT, Simanainen U, Walters KA, Jimenez M, Handelsman DJ. Measurement of sex steroids in murine blood and reproductive tissues by liquid chromatography-tandem mass spectrometry. J Steroid Biochem Mol Biol 2010; 121:611–618.
31. Tomizuka K, Horikoshi K, Kitada R, Sugawara Y, Iba Y, Kojima A, Yoshitome A, Yamawaki K, Amagai M, Inoue A, Oshima T, Kakitani M. R-spondin1 plays an essential role in ovarian development through positively regulating Wnt-4 signaling. Hum Mol Genet 2008; 17: 1278–1291.
32. Mork L, Maatouk DM, McMahon JA, Guo JJ, Zhang P, McMahon AP, Capel B. Temporal differences in granulosa cell specification in the ovary reflect distinct follicle fates in mice. Biol Reprod 2012; 86:37.
33. Maatouk DM, Mork L, Hinson A, Kobayashi A, McMahon AP, Capel B. Germ cells are not required to establish the female pathway in mouse fetal gonads. PLoS One 2012; 7:e47238.

34. Ng A, Tan S, Singh G, Rizk P, Swathi Y, Tan TZ, Huang RY, Leushacke M, Barker N. Lgr5 marks stem/progenitor cells in ovary and tubal epithelia. Nat Cell Biol 2014; 16:745–757.
35. Rastetter RH, Bernard P, Palmer JS, Chassot AA, Chen H, Western PS, Ramsay RG, Chaboissier MC, Wilhelm D. Marker genes identify three somatic cell types in the fetal mouse ovary. Dev Biol 2014; 394: 242–252.
36. Pan H, Cui H, Liu S, Qian Y, Wu H, Li L, Guan Y, Guan X, Zhang L, Fan HY, Ma Y, Li R, et al. Lgr4 gene regulates corpus luteum maturation through modulation of the WNT-mediated EGFR-ERK signaling pathway. Endocrinology 2014; 155:3624–3637.